Electronic Supplementary Material (ESI) for Physical Chemistry Chemical Physics.

Supporting Information

On the Photophysics of Electrochemically Generated Silver Nanoclusters: Spectroscopic and Theoretical Characterization

*Martín I. Taccone,[a,b,c] Ricardo A. Fernandez,[a,b] Franco L. Molina,[a,b,c] Ignacio Gustín,[a,b,c] Cristián G. Sánchez,[d] Sergio A. Dassie[a,b] and Gustavo A. Pino[a,b,c]**

[a] *Departamento de Fisicoquímica, Facultad de Ciencias Químicas, Universidad Nacional de Córdoba, Ciudad Universitaria, Pabellón Argentina, X5000HUA Córdoba, Argentina*

[b] *Instituto de Investigaciones en Fisicoquímica de Córdoba (INFIQC) CONICET-UNC, Ciudad Universitaria, Pabellón Argentina, X5000HUA Córdoba, Argentina.*

[c] *Centro Láser de Ciencias Moleculares, Universidad Nacional de Córdoba, Ciudad Universitaria, Pabellón Argentina, X5000HUA Córdoba, Argentina*

[d] *Instituto Interdisciplinario de Ciencias Básicas, Facultad de Ciencias Exactas y Naturales, Universidad Nacional de Cuyo, CONICET, Padre Jorge Contreras 1300, Mendoza M5502JMA, Argentina.*

**** Corresponding author: E-mail: gpino@fcq.unc.edu.ar; Tel: +54-351-5353866 ext. 53565***

1. Time-Resolved Emission Spectroscopy

Figure S1 shows the time-resolved emission response between 280 nm and 500 nm of the sample containing AgNCs, upon excitation at 267 nm with a diode laser source. A collagen suspension was used to obtain the instrumental response (prompt) at the excitation wavelength. All curves were globally fitted by using deconvolution of the time resolve signal considering 4-exponential decay function leading to the following unique set of excited state lifetimes for all the emission wavelengths explored: $\tau_1 = 1.10$ ns, $\tau_2 = 4.50$ ns, $\tau_3 = 17.1$ ns and $\tau_4 = 0.031$ ns.

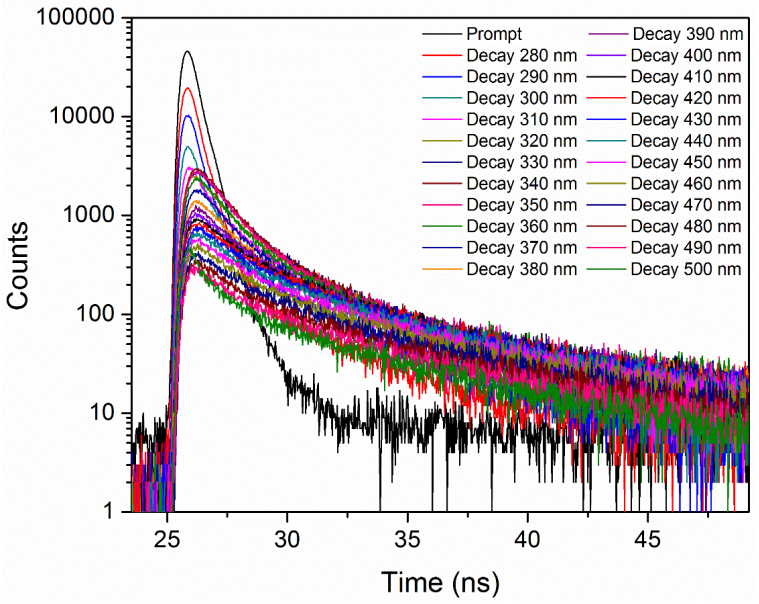

Figure S1: Fluorescence response of the instrument *prompt* (black) and decays (colors) obtained in the TRES experiment at different emission wavelengths upon excitation at 267 nm.

An overall chi-square (χ^2) value of 0.86 was obtained for the global fitting of all the decay curves, which indicates a good quality fit. Table S1 shows the amplitudes factors and the χ^2 values for the individual fittings of each curve of the TRES experiment as a function of the emission wavelength. Above 430 nm the chi-square values fall below 0.8 indicating the poor

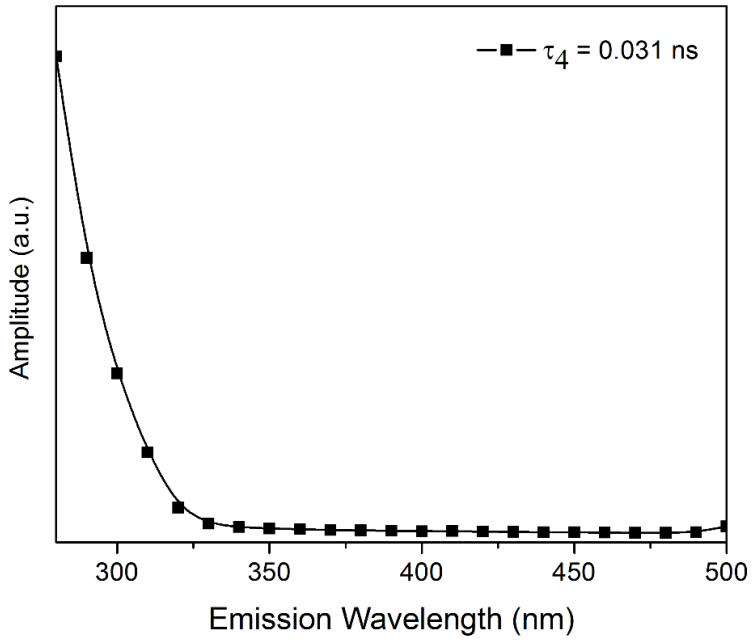

Figure S2: Amplitude (A_4) as a function of the emission wavelength for the lowest lifetime (τ_4) obtained in the global fit of the TRES experiment.

quality of the fitting in this region, which is a consequence of the low signal intensity. Then, the fitting to four exponential decays above 430 nm becomes unreliable and the analysis of the DAS in this spectral region is meaningless.

The quality of the fitting at wavelength < 430 nm was tested by doing the reconvolution of the fluorescence spectrum from the DAS determined by exciting the sample at 267 nm and comparing it with the steady-states fluorescence spectra recorded by exciting at 260 and 270 nm.

The reconstruction of the emission spectrum of the solution from the DAS was performed according to:

$$I(\lambda) = \sum_i F_i(\lambda) = \sum_i A_i(\lambda).\ \tau_i$$

Table S1: Amplitudes associated to the lifetimes and the chi-square (χ^2) values as a function of the emission wavelength obtained in the global fit of the TRES experiment.

Emission wavelength (nm)	A_1	A_2	A_3	A_4	Chi-square (χ^2)
280	(1.7±0.1) x10^{-4}	(1.01±0.02) x10^{-4}	(2.9±0.3) x10^{-6}	(5.880±0.009) x10^{-1}	1.01
290	(2.4±0.1) x10^{-4}	(2.12±0.02) x10^{-4}	(2.5±0.3) x10^{-6}	(3.400±0.007) x10^{-1}	0.84
300	(3.1±0.1) x10^{-4}	(3.02±0.02) x10^{-4}	(1.9±0.3) x10^{-6}	(1.980±0.006) x10^{-1}	0.81
310	(5.2±0.1) x10^{-4}	(3.14±0.02) x10^{-4}	(5.2±0.3) x10^{-6}	(1.010±0.005) x10^{-1}	0.75
320	(7.9±0.1) x10^{-4}	(2.82±0.02) x10^{-4}	(1.22±0.03) x10^{-5}	(3.29±0.03) x10^{-2}	0.90
330	(1.08±0.01) x10^{-3}	(2.24±0.02) x10^{-4}	(2.31±0.04) x10^{-5}	(1.33±0.03) x10^{-2}	0.91
340	(1.26±0.01) x10^{-3}	(1.82±0.02) x10^{-4}	(3.22±0.04) x10^{-5}	(9.0±0.2) x10^{-3}	0.99
350	(1.26±0.01) x10^{-3}	(1.55±0.02) x10^{-4}	(3.67±0.04) x10^{-5}	(7.3±0.2) x10^{-3}	1.04
360	(1.11±0.01) x10^{-3}	(1.40±0.02) x10^{-4}	(3.73±0.04) x10^{-5}	(6.3±0.2) x10^{-3}	1.05
370	(8.88±0.08) x10^{-4}	(1.39±0.02) x10^{-4}	(3.42±0.04) x10^{-5}	(5.2±0.2) x10^{-3}	1.04
380	(6.93±0.08) x10^{-4}	(1.55±0.02) x10^{-4}	(2.85±0.04) x10^{-5}	(4.9±0.2) x10^{-3}	0.98
390	(5.72±0.08) x10^{-4}	(1.81±0.02) x10^{-4}	(2.32±0.04) x10^{-5}	(4.3±0.2) x10^{-3}	0.95
400	(4.96±0.08) x10^{-4}	(2.08±0.02) x10^{-4}	(1.95±0.04) x10^{-5}	(3.9±0.2) x10^{-3}	0.87
410	(4.28±0.07) x10^{-4}	(2.23±0.02) x10^{-4}	(1.64±0.03) x10^{-5}	(3.9±0.2) x10^{-3}	0.86
420	(3.89±0.07) x10^{-4}	(2.16±0.02) x10^{-4}	(1.50±0.03) x10^{-5}	(3.1±0.2) x10^{-3}	0.86
430	(3.25±0.07) x10^{-4}	(2.02±0.02) x10^{-4}	(1.43±0.03) x10^{-5}	(3.0±0.1) x10^{-3}	0.79
440	(2.73±0.06) x10^{-4}	(1.80±0.02) x10^{-4}	(1.31±0.03) x10^{-5}	(2.5±0.1) x10^{-3}	0.75
450	(2.24±0.06) x10^{-4}	(1.56±0.02) x10^{-4}	(1.21±0.03) x10^{-5}	(2.4±0.1) x10^{-3}	0.77
460	(1.84±0.05) x10^{-4}	(1.28±0.02) x10^{-4}	(1.09±0.03) x10^{-5}	(2.3±0.1) x10^{-3}	0.75
470	(1.58±0.05) x10^{-4}	(1.03±0.01) x10^{-4}	(9.3±0.3) x10^{-6}	(1.7±0.1) x10^{-3}	0.69
480	(1.19±0.05) x10^{-4}	(8.4±0.2) x10^{-5}	(8.1±0.3) x10^{-6}	(1.9±0.1) x10^{-3}	0.64
490	(9.4±0.4) x10^{-5}	(6.8±0.1) x10^{-5}	(6.6±0.2) x10^{-6}	(2.6±0.1) x10^{-3}	0.61
500	(5.5±0.4) x10^{-5}	(5.4±0.1) x10^{-5}	(5.0±0.2) x10^{-6}	(9.8±0.1) x10^{-3}	0.62

where $I(\lambda)$ is the fluorescence intensity at each wavelength and $F_i(\lambda)$ is the amplitude factor (A_i) of each component (i) at a given wavelength, weighted by their corresponding decay lifetime (τ_i), that allows comparing the reconstructed spectrum with a steady-state fluorescence spectrum.

Figure S3 shows a comparison of the reconstructed emission spectrum from the TRES results (black squares and full-line) by exciting at 267 nm with the steady-state emission spectra recorded by exciting at 260 nm and 270 nm. The emission spectrum obtained by exciting at 267 nm is expected to fall in between the emission spectra recorded upon excitation at 260

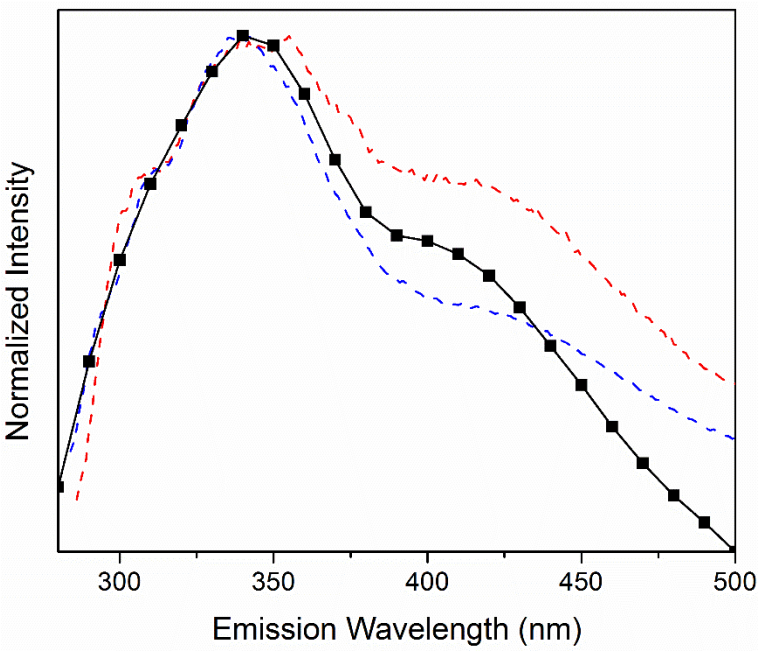

Figure S3: Sum of individual components contribution to the fluorescence response obtained in the TRES experiment with excitation at 267 nm as a functions of the emission wavelength (black squares) and the emission spectra of the sample upon excitation at 260 nm (red) and 270 nm (blue). In all cases the intensities were normalized.

nm and 270 nm. This is true at wavelength below 430 nm, in agreement with the good fitting quality of the TRES results in this spectral region. However, the comparison fails at emission wavelength above 430 nm as expected from the poor quality of the fitting of the TRES in this other spectral region.

2. Mass Spectrometry

The goal of the MS recorded in this work was to get another evidence of the presence of Ag_2, Ag_3^+ and Ag_4^{2+} in the AgNCs solution. Thus, for the sake of clarity, in Figure S4 we report only m/z regions of the mass spectra were chemical species containing these clusters are observed. In addition, the low concentration of AgNCs produced in this work precludes obtaining a clean MS without contamination from other species.

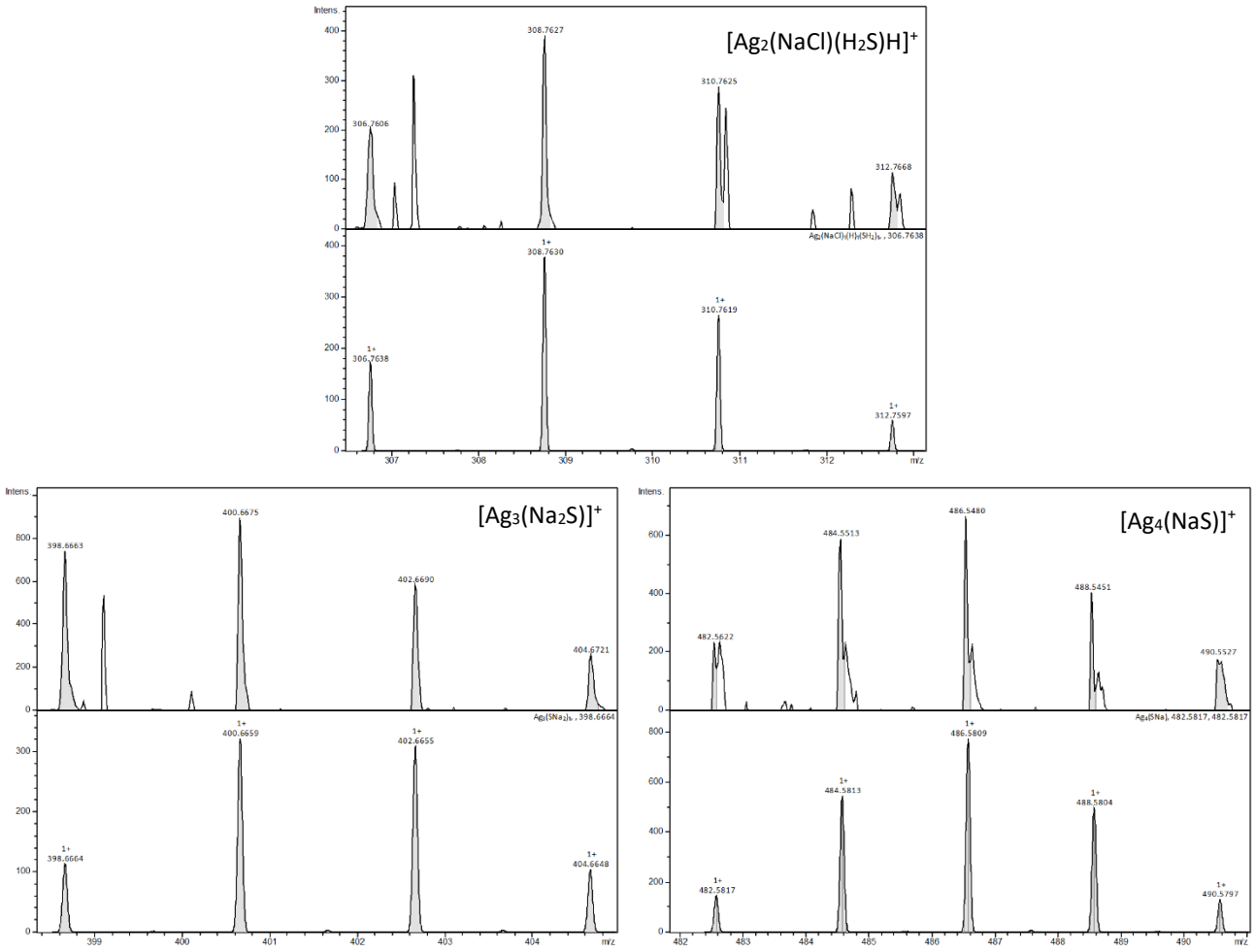

Figure S4: High resolution mass spectra of aggregates with Ag_2 (upper), Ag_3^+ (lower left) and Ag_4^{2+} (lower right) clusters obtained in this work. On each panel, the experimental spectrum (upper) is compare with the simulated isotopic pattern (lower). The aggregates are shown in the upper right corner of each graph.

In all cases, the AgNCs species observed in Figure S4 are complex systems containing sulfide (S^{2-}) moieties in accordance with the precipitant utilized after the synthesis (Na_2S). Nevertheless, the complex containing Ag_2 shows also some chloride (Cl^-) moiety which may be consider an impurity coming from the mass spectrometer, taking into account the low intensity of the signal. These species could be present as stable complexes already in the solution prior the analysis or be produced in the electrospray ionization (ESI) source during the solvent evaporation. In the former case, the optical properties (absorbance, emission and excitation spectra) of the solution should depend strongly on the anion used to precipitate the

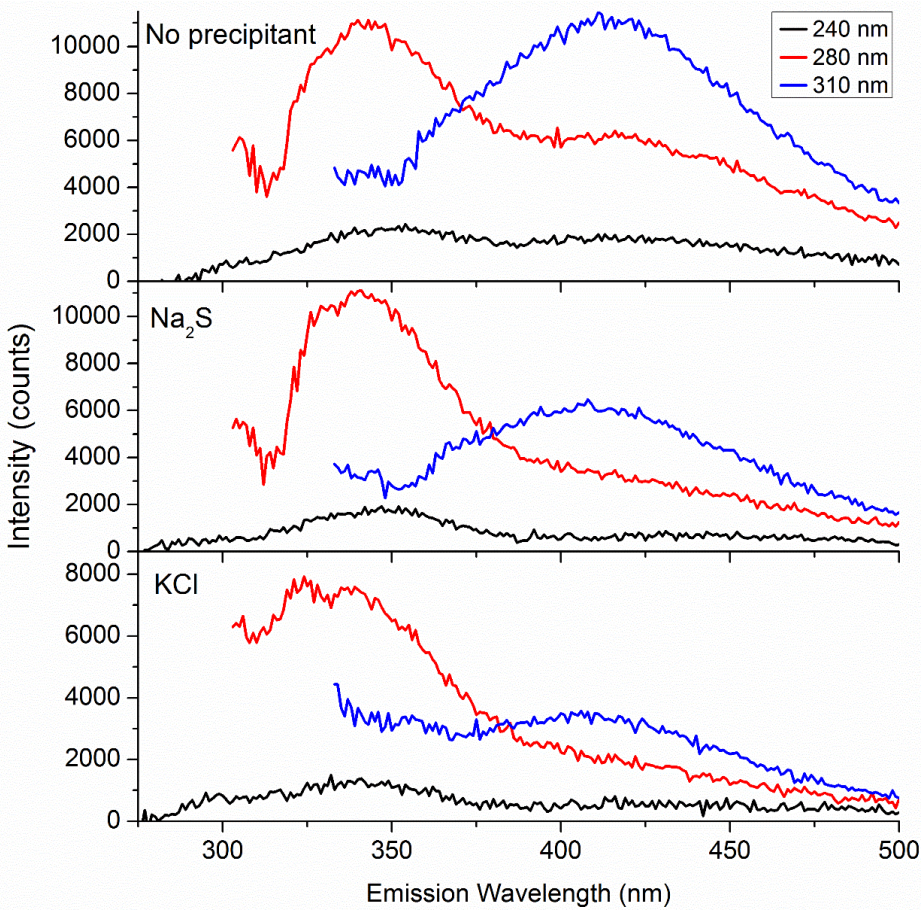

Figure S5: Emission spectra of AgNCs sample excited at 240 nm (black), 280 nm (red) and 310 nm (blue), before and after the addition of either Na_2S or KCl as precipitant

remaining Ag^+. Regarding this, Na_2S and KCl were used as precipitant, prior to the concentration of the sample, to evaluate the anion participation in the optical properties of the sample. The emission spectra at three different excitation wavelengths were obtained before and after addition of the precipitant. Figure S5 shows that the emission bands observed after the synthesis remains unaltered when the precipitant is added, irrespective of the anion used for this purpose. It is also notice that the intensity of the emission band observed at ~ 425 nm upon excitation to all the wavelengths is reduced upon addition of any precipitant. Since this band is observed in all the excitation range it could be associated to another species, which is removed upon addition of the precipitant and further filtering of the dispersion and

whose spectrum is overlapped with the spectra of all the remaining species that are characterized in the manuscript. Further studies are necessary to identify its origin.

It is worth noting that these emission spectra were obtained prior the concentration of the sample, while the spectra presented in the manuscript were all recorded after concentration of the sample to get a better signal to noise ratio. Thus, the intensity of the bands observed in the following figure are approximately 10 times lower than the bands observed in the Figures of the Manuscript.

3. Theoretical Calculations

Table S2: Molecular Orbitals (MOs) contributions, transition energy and oscillator strength of the first 6 excited states of Ag_2

Excited state	Main molecular orbitals contribution	Transition energy eV / nm	Oscillator strength
1	19 → 20 HOMO-LUMO	3.028 / 409.4	0.411
2	18→ 20	4.300 / 288.4	0.000
3	52% (19 → 21) + 45% (16→ 20)	4.397 / 282.0	0.158
4	52% (19 → 22) + 45% (17→ 20)	4.397 / 282.0	0.158
5	52% (16→ 20) + 46% (19→ 21)	4.687 / 264.6	0.295
6	52% (17→ 20) + 46% (19→ 22)	4.687 / 264.6	0.295

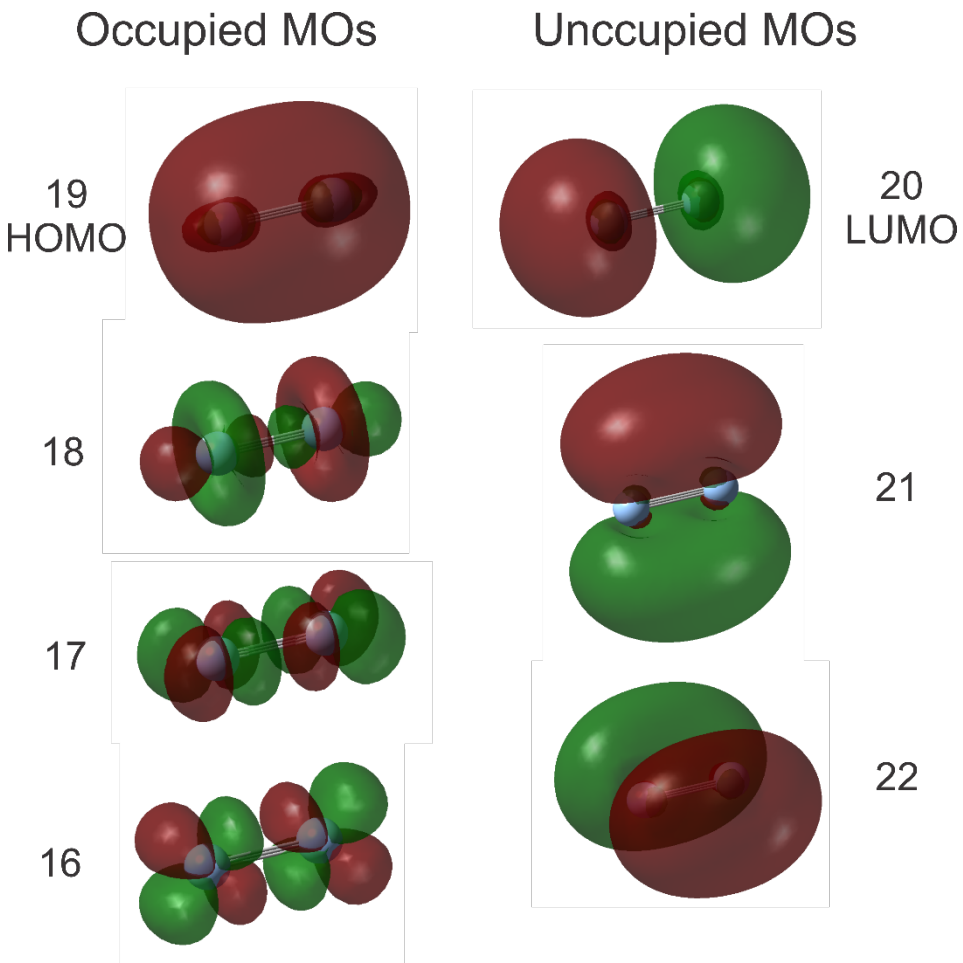

Occupied and unoccupied molecular orbitals (MOs) involved in the 6 firsts electronically excited states of Ag_2 cluster, shown in Table S2. An isovalue of 0.02 was used in all cases. Positive and negative values of the wave functions are indicated as red and green, respectively.

Table S3: Molecular Orbitals, transition energy and oscillator strength of the 6 first excited states of Ag_3^+

Excited state	Main molecular orbitals contribution	Transition energy eV / nm	Oscillator strength
1	61% (28 → 29) + 32 % (28 → 30) 28 HOMO – 29 LUMO)	3.581 / 346.3	0.419
2	32% (28 →29) + 61 % (28 →30)	3.582 / 346.2	0.419
3	41% (27 → 29) + 51 % (27 → 30)	4.716 / 262.9	0.004
4	51% (27 → 29) + 41 % (27 → 30)	4.717 / 262.8	0.004
5	28 → 31	4.792 / 258.7	0.389
6	26 → 30	4.938 / 251.1	0.000

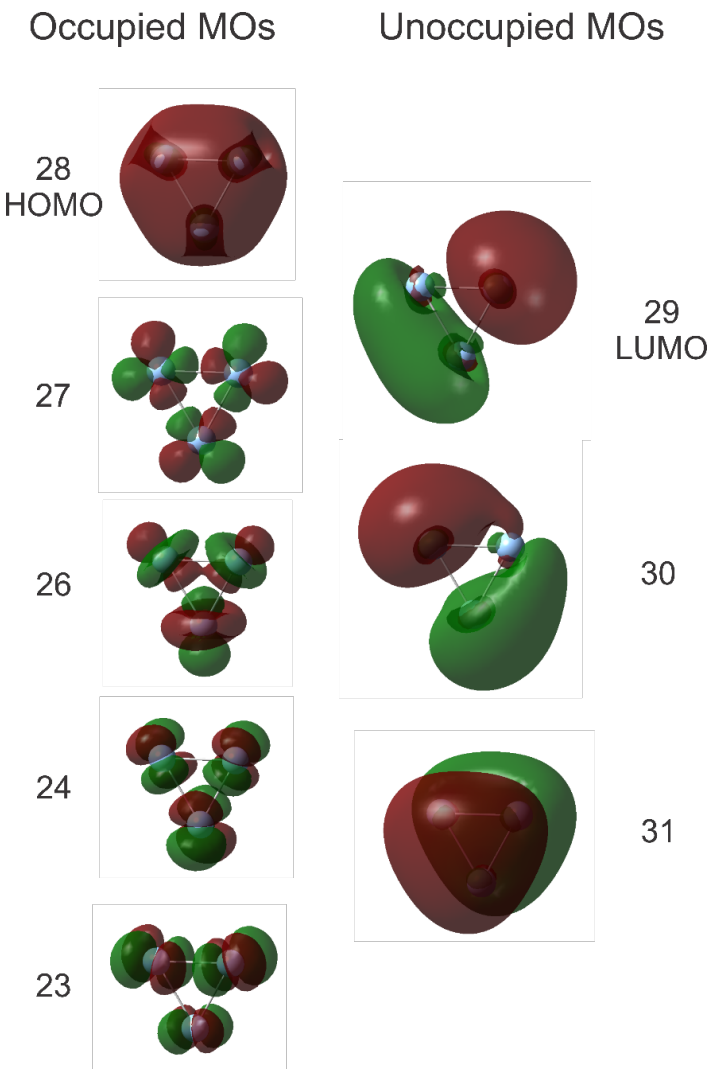

Occupied and unoccupied molecular orbitals (MOs) involved in the 6 first electronically excited states of Ag_3^+ cluster, shown in Table S3. An isovalue of 0.02 was used in all cases. Positive and negative values of the wave functions are indicated as red and green, respectively.

Table S4: Molecular Orbitals, transition energy and oscillator strength of the 5 first excited states of Ag_4^{2+}

Excited state	Main molecular orbitals contribution	Transition energy eV / nm	Oscillator strength
1	37 → 38 HOMO – LUMO	4.131 / 300.1	0.363
2	37 → 39	4.133 / 300.0	0.362
3	37 → 40	4.170 / 297.3	0.359
4	47% (34 → 38) + 46% (35 → 39)	4.918 / 252.1	0.000
5	36 → 40	4.931 / 251.4	0.000

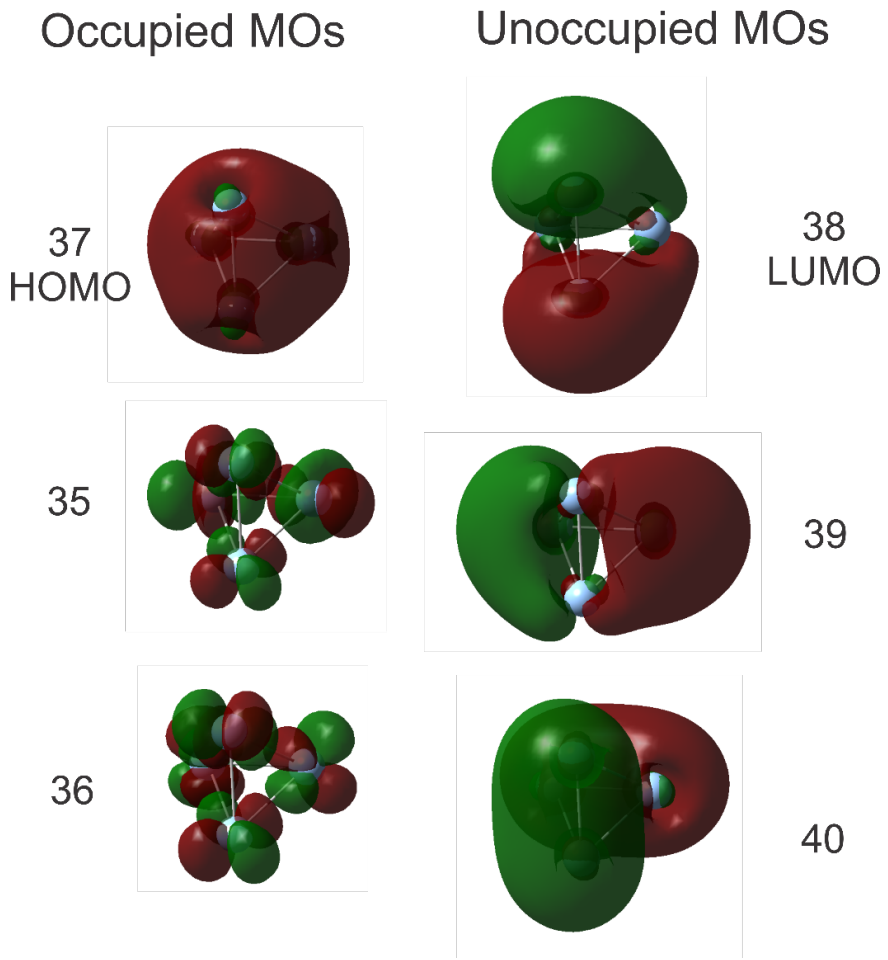

Occupied and unoccupied molecular orbitals (MOs) involved in the 5 first electronically excited states of Ag_4^{2+} cluster, shown in Table S4. An isovalue of 0.02 was used in all cases. Positive and negative values of the wave functions are indicated as red and green, respectively.